


# A PCR-free point-of-care capacitive immunoassay for influenza A virus

Cheng Cheng<sup>1</sup> · Haochen Cui<sup>1</sup> · Jayne Wu<sup>1</sup>  · Shigetoshi Eda<sup>2</sup>

Received: 12 October 2016 / Accepted: 17 February 2017 / Published online: 11 March 2017  
© Springer-Verlag Wien 2017

**Abstract** This article describes a highly sensitive and specific capacitive immunosensor for rapid, low cost and simple-to-use detection of virus particles from clinical swab samples. An inhomogeneous AC electric field is applied on sensor electrodes. This induces positive dielectrophoresis that attracts virus particles to the sensor electrodes. As a result, rapid and sensitive detection of influenza A virus is accomplished without the need for nucleotide isolation and amplification. The same AC signal is used to detect the binding of virus particle to the sensor surface immobilized with the antibody probe. The assay is highly suitable for point-of-care use. When testing clinical swab samples, the response of samples at various dilutions is analyzed, and an optimal dilution is found and used for subsequent blind tests of clinical swab samples. Analytical experiments on standard influenza virus sample demonstrate a limit of detection of  $0.25 \text{ pg}\cdot\text{mL}^{-1}$ . Other figures of merit include (a) an assay time of 30 seconds; (b) a diagnostic sensitivity of 90%; and (c) a specificity of 70%. Blind tests are conducted for a panel of twenty nasal swab samples, and the results are in good agreement with those by using the commercial reverse transcription polymerase chain reaction.

**Keywords** Alternating current electrokinetics · Interfacial capacitance · Dielectrophoresis · Microelectrode

## Introduction

Influenza is a very common infectious disease. While it usually causes only mild illness, it can be life-threatening for infants, elderly and immunodeficient people. Worldwide, seasonal influenza is estimated to result in 250,000–500,000 deaths per year [1]. Worldwide human health has been challenged by pandemic threats including the emergence of highly pathogenic influenza A virus from mutation of avian influenza or other animal reservoirs. Timely detection of influenza is critically important, which can shorten the delay in treatment, reduce the duration of hospitalization, and improve the quality of patient care.

Accurate diagnosis of influenza virus is done by either virus isolation detection of virus-specific antibodies [2] or genomic detection by reverse-transcription quantitative polymerase chain reaction (RT-qPCR) [3]. Conventional viral tissue cell culture approach has been used for viral disease diagnosis for decades, but the isolation of viral pathogens in cell culture is usually slow (3–10 days) and requires technical experience [4]. Shell vial assays can reach cell culture diagnostic results faster (3 days) than conventional cell culture method, except for that shell vial assays lack the ultimate sensitivity (60% sensitivity versus 94% in conventional culture). So rapid cell culture method still requires conventional cell cultures to assure the diagnosis sensitivity [5]. Nowadays, diagnostics by RT-qPCR is routinely done in many laboratories for detection of RNA viruses, such as influenza A, which yields results in hours and is used increasingly for early diagnosis. However, RT-qPCR has a high risk of sample contamination despite its being operated by trained operators, and it

---

**Electronic supplementary material** The online version of this article (doi:10.1007/s00604-017-2140-4) contains supplementary material, which is available to authorized users.

---

✉ Jayne Wu  
jaynewu@utk.edu

<sup>1</sup> Department of Electrical Engineering and Computer Science, The University of Tennessee, 1520 Middle Drive, Knoxville, TN 37996, USA

<sup>2</sup> Department of Forestry, Wildlife and Fisheries, The University of Tennessee Institute of Agriculture, 2431 Joe Johnson Drive, Knoxville, TN 37996, USA

requires good financial and technical resources to perform, is often restricted to central laboratories. The tests discussed above require relatively expensive equipment, skilled examiners, and at least several hours to get a result. These disadvantages delay the decision-making process and prevent their use in resource-limited settings.

A rapid point-of-care (POC) diagnosis for infectious diseases is desired and will have significant impact on the healthcare. Rapid Influenza Diagnostic Tests (RIDTs) are commercially available POC tests for early detection of influenza. They have high specificity, however their sensitivity is modest (62.3%) and highly variable with a reasonable likelihood of producing false negative diagnosis. Hence, similar to other diagnostic tests that need confirmation, RIDTs are often inconclusive until further laboratory testing through rt-PCR in specialized diagnostic laboratories [6]. In addition, RIDTs are not quantitative. Therefore, a new rapid, sensitive and quantitative POC detection method for influenza A (or many other viruses) is highly desired for effective control of the outbreak and spread of diseases.

One major thrust for biosensor research is to develop POC diagnostics. Table 1 shows a summary of biosensor methods for influenza virus detection and their performances. Types of biosensors mainly include electrochemical [7] and optical sensors (such as surface plasmon resonance, SPR [8], or with luminescence resonance energy transfer, LRETSPR [9]), within which there are many variations in the instrument designs. Another relatively convenient and desirable alternative is impedance immunosensors which detects binding of influenza virus by using electrochemical impedance spectroscopy with interdigitated microelectrodes [10]. Typically, in an impedance immunosensor, the detection is based on the increase in the charge transfer resistance ( $R_{ct}$ ) due to specific binding at the electrode surface. To separate  $R_{ct}$  from other components in the sensor impedance, multiple steps and special measuring buffers are usually needed, such as baseline measurement, sample incubation, washing, sometimes air drying, and measurement and data extraction. Extraction of  $R_{ct}$  is often a subjective process, prone to human intervention, affecting the robustness of detection results. Being label-free, thus eliminating the need for labeling (fluorescent, chemical, or radioisotope) target molecules, is also important. While considerable research effort has been devoted to biosensors for

diagnosis at the bedside or in the clinic, there are few POC devices being routinely used in real applications. Successful POC diagnostic systems require the following critical attributes: sufficient sensitivity, robustness, simple test procedure and short sample-to-result time.

In our previous study, we presented a label-free, highly sensitive and specific affinity-sensing technology that can be performed rapidly (1 min from sample to result) by a lay person with a single-step and no wash operation. This technology is called alternating current electrokinetics (ACEK) capacitive sensing method [11, 12]. As shown in Fig. 1a, interfacial capacitance between the electrode and the sample fluid is used to quantify biomolecular deposition or capture on functionalized microelectrodes' surface, and a detection protocol is developed to obtain interfacial capacitance directly without complicated data interpretation. Capacitive affinity sensors were reported in the past for virus detection [13, 14], however, they used bulk capacitance which is in parallel to the impedance of bulk solution. As a result, the detection results were strongly affected by matrix effect. To achieve specificity, in conventional capacitive biosensors, a reference signal was needed from a control test to subtract background signal. Additionally, in the two reports, target viruses were prepared and measured in standard buffers such as phosphate-buffered saline buffer,  $\text{KH}_2\text{PO}_4/\text{K}_2\text{HPO}_4$  buffer or  $\text{Na}_2\text{HPO}_4/\text{KH}_2\text{PO}_4$  buffer instead of complex fluids, due to limited specificity from measuring bulk capacitance. In comparison, interfacial capacitance ( $C_{int}$ ) can reflect with high sensitivity and specificity any topological changes such as molecular deposition at the sensor surface, as  $C_{int}$  can be isolated easily from the resistance of bulk solution.

Another feature of ACEK capacitive sensing is the acceleration of detection and improved sensitivity from ACEK effects incorporated into capacitive measurement. Conventional biosensors including impedimetric and capacitive sensors suffer from long response time and low sensitivity, because they rely on Brownian movement for target bioparticles to randomly move to the binding sites on electrodes. To break diffusion barrier, ACEK capacitive sensing method uses an AC signal capable of inducing ACEK effects to interrogate the interfacial capacitance on microelectrodes. In this method, interdigitated microelectrodes (as shown in Fig. 1b) functionalized with analyte-specific probes (antibody here) is employed as

**Table 1** Overview of influenza virus detection by biosensors

Method	Label free	Limit of detection	Time
Electrochemical nuclei acid detection after RT-PCR [7]	√	7.5 pg·mL <sup>-1</sup>	15 min
Optical (SPR) [8]	√	20 ng·mL <sup>-1</sup>	1 h
Optical (LRETSPR) [9]	×	7.7 pg·mL <sup>-1</sup>	2 h
Impedance immunosensor [10]	×	10 pg·mL <sup>-1</sup>	30 min
This technique	√	0.25 pg·mL <sup>-1</sup>	30 s

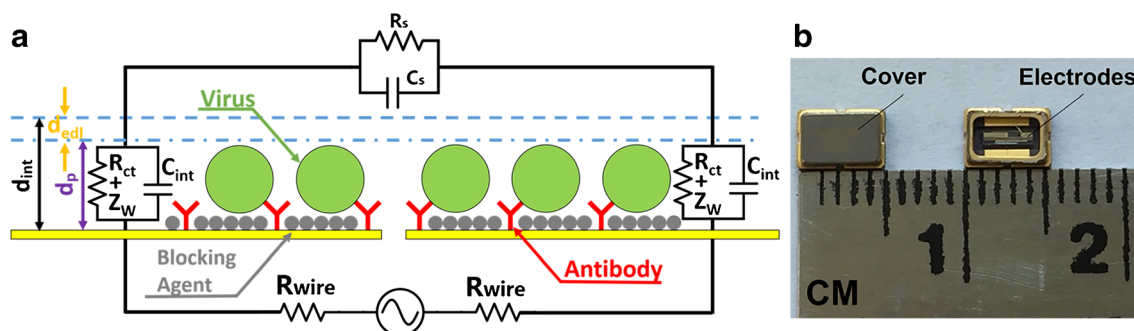


**Fig. 1** (a) Capacitive sensing mechanism and equivalent circuit of (b) the commercially available surface acoustic wave (SAW) electrode chip

sensors, and low voltage AC signal is applied over the microelectrodes to induce ACEK effect attracting analytes towards the electrode surface and accelerating the binding to immobilized probe molecules, which takes place concurrently with the measurement of interfacial capacitance.

Since its advent in late 1990s, ACEK has been investigated by many researchers to accelerate the travel of macromolecules towards sensing areas, and improvement in sensor responses has been observed after applying ACEK effects [15–17]. Several kinds of ACEK effects can occur [18, 19] when an inhomogeneous AC electric field is applied through microelectrodes to an aqueous solution. Directed particle movement can be caused by dielectrophoresis (DEP) [20], and particle can also be carried by microflows such as AC electroosmosis (ACEO) [21] or AC electrothermal (ACET) flows [17, 22–24] to reach the microelectrodes. However, in almost all the existing label free ACEK devices, the amplitude of AC signal used is usually in the range of 10 V, and the ACEK concentration step is separate from the detection step [17, 25, 26]. Applying a  $\sim 10$  V voltage over biofluids raises the concerns of electrolysis, biofouling, etc. Steps such as separate pre-concentration and possibly labeling would increase the complexity and time of sensor operation. These reasons severely limit the use of ACEK in biosensing. In contrast, ACEK capacitive sensing method is a rapid, single-step operation without any wash steps. Low voltage ( $<1$  V) AC electrokinetic (ACEK) effects for bioparticle enrichment and label-free measurement of interfacial capacitance ( $C_{int}$ ) are conducted simultaneously by using the same AC signal.

This method was used in a series of proof-of-concept experiments detecting specific protein biomarker, pathogens, small molecules, etc. [11, 12, 27, 28]. For influenza A virus detection, the method uses a commercially available interdigitated microelectrode array shown in Fig. 1b at a cost of  $\sim \$0.80$  USD per test. It is simple to use by users. All it takes is to read the sensor capacitance continuously at an optimized ACEK frequency and voltage. With a response time of 30 s, we demonstrated a limit of detection (LOD) of  $0.25 \text{ pg}\cdot\text{mL}^{-1}$  and diagnostic sensitivity of 90% and specificity of 70% for 20 clinical swab samples when bench-marked against an Xpert® Flu by Cepheid (based on RT-qPCR).

## Experimental section

### Buffer and sample preparation

Sample solution in this work is prepared using as  $0.1\times$ PBS (1 mM phosphate-buffered saline [pH 7.0] containing 15 mM sodium chloride) with a conductivity of  $0.15\text{--}0.16 \text{ S/m}$  ( $600\text{--}700 \Omega\cdot\text{cm}$ ).  $0.1\times$ PBS containing  $0.05 \text{ v/v}\%$  Tween 20 (Fisher Scientific, Pittsburgh, PA, <https://www.fishersci.com/us/en/home.html>), called  $0.1 \times \text{PBS-T}$ , is used as the dilution buffer for testing.  $0.1\times$  buffer B is  $0.1\times$  PBS-T containing  $10 \text{ v/v}\%$  SuperBlock (Pierce Biotechnology, Rockford, IL, <https://www.thermofisher.com/us/en/home/brands/thermo-scientific/pierce-protein-biology.html>) and is used as the blocking reagent. The chemical linker used for improving surface functionalization with antibody is  $10 \text{ v/v}\%$  3-aminopropyltriethoxysilane (APTES, Thermo Scientific, Waltham, MA, <http://corporate.thermofisher.com/en/home.html>) in absolute ethanol and  $2.5\%$  glutaraldehyde in water. Antibody solution used for electrodes functionalization is  $41.5 \mu\text{g}\cdot\text{mL}^{-1}$  anti-influenza A antibody in distilled water.

Antibody used as negative control is  $40 \mu\text{g}\cdot\text{mL}^{-1}$  bovine IgG whole molecule (Johnson ImmunoResearch, West Grove, PA, <https://www.jacksonimmuno.com>) in water. In this paper, the electrode coated with negative control antibody is termed dummy electrode. Spiked influenza A virus samples are  $1.525$ ,  $0.1552$  and  $0.01525 \mu\text{g}\cdot\text{mL}^{-1}$  of influenza A virus suspended in  $0.1\times$ PBS-T. Clinical nasal swab samples are preserved in M4RT (Remel, KS, <http://www.remel.com/Home.aspx>) and is diluted up to  $1:100,000$  using  $0.1\times$ PBS-T. Level of virus in the clinical swab samples are assessed by RT-qPCR.

### Microelectrode sensors

The electrode chips are modified from AVX Corps' PARS 433.92 Surface Acoustic Wave (SAW) chip. The metal cover of the SAW resonator is removed mechanically to expose the working electrode array for use, as shown in Fig. 1b. The sensor consists of aluminum interdigitated electrodes deposited on quartz substrate. Each electrode finger is  $2.0 \mu\text{m}$  wide,

170  $\mu\text{m}$  long, with 2.0  $\mu\text{m}$  spacing from each other. The metal housing around the electrode chip is about 4 mm (L)  $\times$  2.5 mm (W)  $\times$  1 mm (H), and accommodates  $\sim$ 10  $\mu\text{L}$  of sample. The interdigitated electrodes are electrically connected to two contact pads on the chip bottom, which are then connected to an impedance analyzer (Agilent 4294A, <http://www.agilent.com/home>).

### Sensor cleaning

Electrode preparation includes exposing and cleaning the electrodes, and surface functionalization with probe molecules to achieve specificity. Prior to incubation with linker and probe molecules, the microelectrode chip is thoroughly cleaned by washing with acetone, isopropyl alcohol and de-ionized water, and then treated with ozone. The surface quality is closely monitored by measuring the  $C_{int}$  [29].

### Sensor functionalization

After the electrode cleaning, electrode surface is functionalized with probe molecules to achieve specificity. The 3-aminopropyltriethoxysilane (APTES)-mediated method is used to improve binding or adhesion between organic polymers and metal substrates [30]. The electrodes are immersed in 10% APTES in ethanol for 15 min and then baked at 125  $^{\circ}\text{C}$  for 30 min. After the electrodes cool down to room temperature, 2.5% glutaraldehyde in water is added onto electrodes, which then are left at room temperature for 1 h. After the probe (antibody) immobilization, to minimize non-specific binding, the electrodes are further treated with blocking agent (0.1 $\times$ buffer B) for 30 min. This blocking step is taken to block unoccupied aldehyde groups of glutaraldehyde molecules.

### Measurement

Based on our prior work on ACEK capacitive sensing of bioparticles [12], our experiments use an AC frequency range between 1 kHz and 1 MHz, which is much lower than the SAW chip's resonant frequency of 433.92 MHz, so no piezoelectric effects need to be considered in our experiments. Electrodes functionalized as described above are loaded with a viral suspension and connected to an impedance analyzer for measurement. A high precision impedance analyzer (Agilent<sup>®</sup> 4294A) is used for applying the AC signal and simultaneously measuring the capacitance change. Each test data point is run with 5 replicates. Least square linear fitting algorithm is performed to determine the capacitance change rate.

## Results and discussion

### Direct capacitance measurement

In this work, the interfacial capacitance is sensed and used as an indicator of probe-analyte binding. As shown in Fig. 1a, the interfacial capacitance can be defined as

$$C_{int} = A_{int} / \left( \frac{1}{\varepsilon_p} d_p + \frac{1}{\varepsilon_s} d_{edl} \right) \quad (1)$$

where  $\varepsilon_s$  and  $\varepsilon_p$  are permittivities of the solution and bioparticle, respectively,  $A_{int}$  is the surface area of the interfacial capacitor of the functionalized electrode,  $d_p$  and  $d_{edl}$  are the thickness of biomolecular deposition and electric double layer formed on the electrodes surface respectively. With binding process continuing, the thickness of interfacial layer,  $d_{int}$ , keeps increasing which leads to a decrease of  $C_{int}$ . By monitoring the change rate of  $C_{int}$ , specific binding of analyte with probe molecules can be detected. Additionally, using  $C_{int}$  improves the sensor specificity, as illustrated by an equivalent circuit in Fig. 1a, which consists of the electrode's self-resistance ( $R_{wire}$ ), interfacial capacitance ( $C_{int}$ ), charge transfer resistance ( $R_{ct}$ ), Warburg coefficient ( $Z_W$ ), fluid bulk resistance ( $R_s$ ) and dielectric capacitance of the electrode cell ( $C_s$ ). The effect of interfering constituents and undesired electroactivity in a complex fluid mostly shows up through the fluid resistance  $R_s$ , which can be easily eliminated when we only measure  $C_{int}$ . Consequently, high specificity can be achieved, and no wash step is required for our sensing method.

In order to measure  $C_{int}$  directly, the sensor impedance should be able to be simplified as a serial connection of  $R$  and  $C$  at the measuring frequency. At the measuring frequency,  $C_{int}$  should pose a much smaller impedance than  $R_{ct}$ , and  $C_s$  is negligible, i.e.  $C_s$  poses a higher than impedance than  $R_s$ . Furthermore, ACEK effects at this frequency should help surface binding [12]. The measured and fitted impedance spectrum can be found in Fig. S1(b) of the supporting information. The fitted values of the equivalent circuit elements are found as follows:  $C_{int} = 40$  nF,  $R_{ct} = 10$   $\Omega$ ,  $Z_W = 270$  k $\Omega$ ,  $R_s = 1500$   $\Omega$  and  $C_s = 3.2$  pF. Our prior work using optical detection found that, at 100 kHz, binding enhancement by ACEK effects was the most pronounced [31]. Here, it was found that around the frequency of 100 kHz, the circuit can be simplified as  $R_s$  in serial with  $C_{int}$ . Hence, 100 kHz is chosen as the working frequency. At this frequency, the impedance of interfacial capacitance is calculated to be 39.79  $\Omega$ . As a result, 2.576% of the total applied AC signal ( $\sim$ 0.26 mV) is applied over the interface and 97.101% ( $\sim$ 9.70 mV) on the bulk solution. Therefore, there is very little electrical stress on immobilized probe molecules, and the majority of the applied electric field is used to induce DEP for bioparticle enrichment.

## Proof of concept

Experiments are conducted to test the capability of the capacitive immunosensor. The measuring signal is 10 mV, 100 kHz AC signal. 0.1×PBS-T and 1.52 ng·mL<sup>-1</sup> influenza A virus is tested on functionalized electrodes as control and positive tests, and 152.5 ng·mL<sup>-1</sup> influenza A virus sample on dummy electrodes as negative test. Prior work has shown that biological samples based on 0.1×PBS is compatible with protein-protein interactions to detect high affinity interaction of antibody-antigen pair [11]. Here, a slightly different buffer system, 0.1×PBS-T, is used here to improve specificity. Added non-ionic detergents do not affect the affinity of interactions between antibody and viral protein. It is expected to enhance the specificity of our assay. Firstly, detergents are known to reduce non-specific binding of protein to surfaces. Secondly, virus in clinical swab samples may become clustered with other particles presented in the bodily fluid, which may block the interaction between virus and antibody. Detergents can help to dissociate the virus from those interfering particles and enhance the sensitivity of the assay.

Figure 2 shows the representative changes of normalized interfacial capacitance  $|C_{int}|$  with time for positive, negative and control samples. Normalized interfacial capacitance  $|C_{int}|$  is found with respect to the  $C_{int}$  of each sample at initial time point. Therefore, problems with baseline drift or the need for a reference sensor can be avoided, greatly simplifying the detection procedure and instrumentation. Furthermore, it also relaxes the requirements on instrument precision, and minimizes the effect of difference between sensors. To quantify the changes in  $C_{int}$ , the percentage change of normalized  $|C_{int}|$ ,  $d|C_{int}|/dt$  in %·min<sup>-1</sup>, is adopted as the detection metric and used for the remainder of this work. The capacitance values of the control and negative tests stay rather constant, yielding near zero

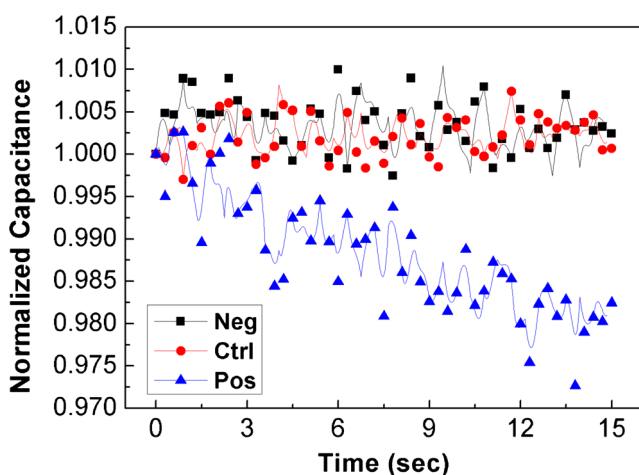


**Fig. 2** Capacitance change of tests with negative (152.5 ng·mL<sup>-1</sup> influenza A virus sample on dummy electrodes), control (0.1×PBS-T on functionalized electrodes) and positive tests (1.52 ng·mL<sup>-1</sup> influenza A virus on functionalized electrodes)

capacitance change rates, 0.11 and 0.50%·min<sup>-1</sup>, respectively. The positive test leads to a change rate of -6.52%·min<sup>-1</sup>, which can be clearly differentiated from the negative and control tests. As shown in Eq. 1 previously, the decrease on interfacial capacitance is due to the increase of thickness of interfacial layer caused by binding reaction on the surface.

## Testing condition optimization

An important component of ACEK capacitive sensing is the induction of ACEK effects during capacitive sensing, which attract target bioparticles towards sensor. ACEK includes DEP, ACEO and ACET effect. This work mainly utilizes positive DEP for enrichment of bioparticles around electrodes. DEP is caused by interactions between a particle's dipole moment and a non-uniform field [18]. This technique has been studied in great details for controlled manipulation of particles, binary separation, and characterization of particles. The DEP velocity on a spherical particle can be described as follows [18]

$$u_{DEP} = \frac{\varepsilon_m a^2}{6\eta} \operatorname{Re} \left[ \frac{\varepsilon_p^* - \varepsilon_m^*}{\varepsilon_p^* + 2\varepsilon_m^*} \right] |\nabla|E|^2$$

$$= \frac{\varepsilon_m a^2}{6\eta} \operatorname{Re}[K(\omega)] |\nabla|E|^2 \quad (2)$$

where  $\varepsilon_m$  is the medium permittivity,  $a$  is the radius of the particle,  $\varepsilon_p^*$  and  $\varepsilon_m^*$  are particle and medium complex permittivity respectively. Complex permittivity is defined as  $\varepsilon^* = \varepsilon - j \frac{\sigma}{\omega\varepsilon}$  (where  $\sigma$  is conductivity and  $\omega$  is angular frequency).  $K(\omega)$ , a function of  $\omega$ , is known as Clausius–Mossotti factor. Therefore, the DEP velocity  $u_{DEP}$  is frequency dependent. The real part of the Clausius–Mossotti factor is a determining factor for DEP velocity on a particle. For  $\operatorname{Re}[K(\omega)] > 0$ , positive DEP (pDEP) happens, particles are attracted to electrodes, while for  $\operatorname{Re}[K(\omega)] < 0$ , negative DEP (nDEP) happens, particles are repelled from electrodes. In this work, pDEP will be induced to accelerate the binding reaction between virus and antibody. Usually pDEP happens when the particle conductivity is higher than the fluid conductivity. In Ref. [17], pDEP of *E.coli* bacteria was observed in a solution with ~1 S/m conductivity (much higher than in this work) at 300 kHz. There is also prior report inducing pDEP for virus particles under similar fluid conductivity and AC signals [32]. Using optical detection, our prior work also observed DEP enrichment of antibodies and DNA molecules at 100 kHz [31, 33]. So it is expected that influenza A virus particles will experience positive DEP at 100 kHz.

Accompanying DEP, the other two ACEK effects, AC electroosmosis (ACEO) and AC electrothermal (ACET) effects, will also be induced by an AC signal to various degree. ACEO and ACET effects generate microflows that can carry small biomolecules, and effective enrichment of biomolecules for detection has been realized by ACEO [34] and ACET

effect [25]. As DEP effect depends on the size of biomolecules, while ACEO or ACET effect is size independent, the relative importance of ACEK effects varies with the size of target molecules. In [25], both ACET and DEP were shown to be important for enriching DNA molecules of 150 base-pairs (~48 k Dalton). Under the same conditions used in this work, prior experimental work observed that DEP is dominant for biomolecules comparable to antibodies (~150 k Dalton) or larger [24]. For this work, the target analyte is influenza A virus particle, which is much larger than antibodies, so DEP should be the major enrichment mechanism. Order of magnitude estimation of ACEK velocities using equations in our previous work [34] and a diameter of 100 nm for virus particle found the DEP and ACET velocities for influenza A virus particles to be  $3.87 \times 10^{-9}$  and  $7.61 \times 10^{-13}$  m·s<sup>-1</sup> respectively, in qualitative agreement with the experimental results.

To elucidate the effects of ACEK mechanisms on detection, the first set of experiments is to find out the effect of AC frequency on the sensor response. Based on Eq. 2, DEP effects are frequency-dependent. AC signals of various frequencies at 10 mV are used to measure the capacitance changes from influenza A virus samples at a concentration of  $1.525 \text{ ng}\cdot\text{mL}^{-1}$ . The measured capacitance change rates are given in Fig. 3a. The

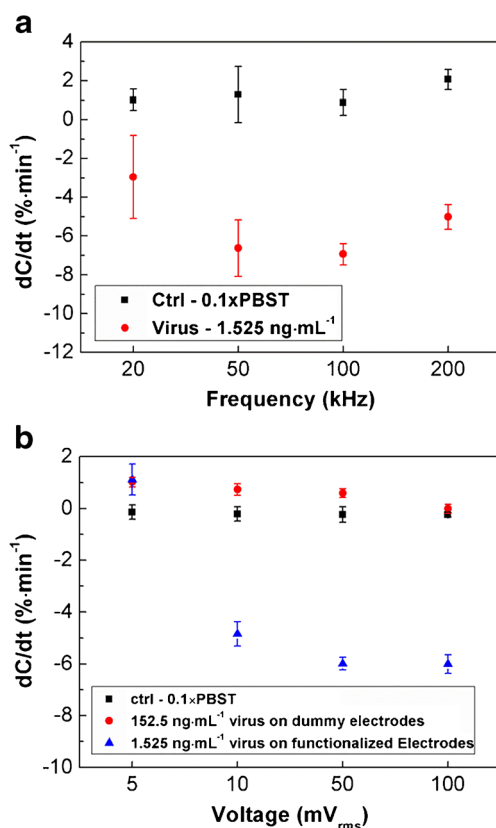


**Fig. 3** Responses of  $0.1 \times \text{PBS-T}$ ,  $1.52 \text{ ng}\cdot\text{mL}^{-1}$  influenza A virus on functionalized electrodes, and  $152.5 \text{ ng}\cdot\text{mL}^{-1}$  influenza A virus sample on dummy electrodes (a) when using  $10 \text{ mV}$  AC signal with its frequency varied from 20 to 200 kHz and (b) when using  $100 \text{ kHz}$  AC signal with its voltage varied from 5 to  $100 \text{ mV}$

response shows a bell-shape dependence on AC frequency, with its optimal frequency between 50 and  $100 \text{ kHz}$ , which indicates that the DEP is the dominant enrichment mechanism. Consequently, AC signal at  $100 \text{ kHz}$  is used in all the subsequent experiments.

Next, AC voltages varying from  $5 \text{ mV}$  to  $100 \text{ V}$  are used to measure  $1.52 \text{ ng}\cdot\text{mL}^{-1}$  influenza A virus sample on functionalized electrodes. The background blank buffer, which is  $0.1 \times \text{PBS-T}$ , is also tested on the functionalized electrodes from 5 to  $100 \text{ mV}$  as control. Negative control experiments with  $152.5 \text{ ng}\cdot\text{mL}^{-1}$  influenza A virus sample are measured under the same voltage conditions on dummy electrodes (electrodes without antibody). Experiments with each voltage are repeated three times.

As shown in Fig. 3b, responses of the  $0.1 \times \text{PBS-T}$  control samples on functionalized electrodes and  $152.5 \text{ ng}\cdot\text{mL}^{-1}$  influenza A virus sample on dummy electrodes remain quite small through the voltage range of  $5\text{--}100 \text{ mV}$ , with a limited response ranged from  $-0.14$  to  $-0.24$  and  $1.02$  to  $-0.01\% \cdot \text{min}^{-1}$ . For tests on functionalized electrodes, due to DEP effect, the capacitive response decreases as the voltage increases from 5 to  $100 \text{ mV}$ , indicating that more binding takes place with higher AC voltage. When the voltage level is above  $10 \text{ mV}$ , the increase of sensor's response becomes limited due to saturation of binding sites on the sensor. Therefore,  $10 \text{ mV}$  is chosen as the measuring voltage. At this voltage, DEP effect will be weak for particles smaller than virus such as protein to cause appreciable capacitance change [12], therefore improved the sensor specificity in complex matrix.

#### Dose response and limit of detection (LOD)

Dose response of influenza A virus samples in various concentrations ( $15.25$ ,  $152.5 \text{ pg}\cdot\text{mL}^{-1}$ ,  $1.525$ ,  $15.25$  and  $152.5 \text{ ng}\cdot\text{mL}^{-1}$ ) is shown in Fig. 4. All tests are repeated four times and the averaged responses of  $dC/dt$  are  $-2.72$

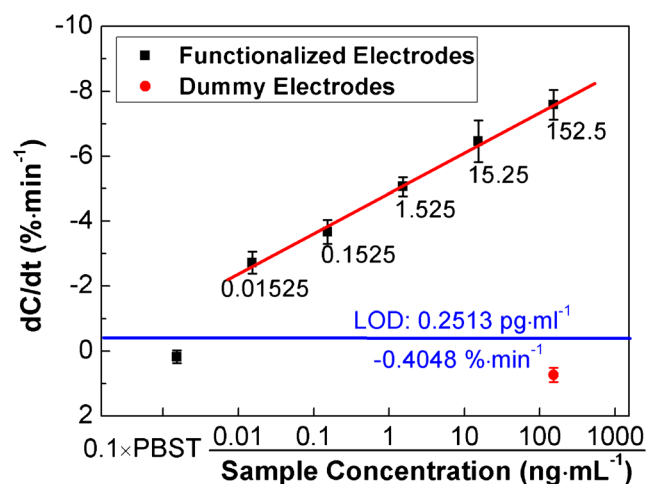


**Fig. 4** Dose response of influenza A samples as a function of concentration with an LOD of  $0.2513 \text{ pg}\cdot\text{mL}^{-1}$

$\pm 0.34\% \cdot \text{min}^{-1}$  for  $15.25 \text{ pg} \cdot \text{mL}^{-1}$  virus sample,  $-3.67 \pm 0.37\% \cdot \text{min}^{-1}$  for  $152.5 \text{ pg} \cdot \text{mL}^{-1}$ ,  $-5.06 \pm 0.29\% \cdot \text{min}^{-1}$  for  $1.525 \text{ ng} \cdot \text{mL}^{-1}$ ,  $-6.46 \pm 0.64\% \cdot \text{min}^{-1}$  for  $15.25 \text{ ng} \cdot \text{mL}^{-1}$  and  $-7.59 \pm 0.46\% \cdot \text{min}^{-1}$  for  $15.25 \text{ ng} \cdot \text{mL}^{-1}$ . Responses of control tests and dummy electrodes are  $0.18 \pm 0.19$  and  $0.73 \pm 0.23\% \cdot \text{min}^{-1}$  respectively, which can be easily differentiated from the responses of functionalized electrodes. Linear fitting line of the dose response is expressed by Eq. (3) with a correlation coefficient ( $R^2$ ) of 0.994.

$$\frac{dC}{dt} (\% \cdot \text{min}^{-1}) = -1.236 \cdot \lg(x(\text{ng} \cdot \text{mL}^{-1})) - 4.855 \quad (3)$$

where  $x$  is sample concentration in  $\text{ng} \cdot \text{mL}^{-1}$ .

LOD is defined as three times the standard deviations ( $0.5816\% \cdot \text{min}^{-1}$ ) from the background response, which is  $0.1 \times \text{PBS-T}$  ( $0.1769\% \cdot \text{min}^{-1}$ ). The LOD, also the threshold value for differentiating the positive samples from the negative, is calculated to be  $-0.4048\% \cdot \text{min}^{-1}$  which corresponds to  $0.2513 \text{ pg} \cdot \text{mL}^{-1}$  influenza A virus.

### Experiments with clinical swab samples

It is common practice to dilute clinical samples in standard buffer. Due to the complexity of clinical samples, highly diluted samples can reduce non-specific binding, which improve the selectivity of the sensor. With more dilution of clinical samples, chances of false positive results can be reduced. However, sensor's sensitivity will also suffer since the concentration of target particles is reduced at the same time. The optimization dilution factor helps to decide which dilution can be used for the blind tests of unknown swab samples in the next step. In addition, unlike the spiked samples in previous sections, clinical swab samples are in M4RT instead of  $0.1 \times \text{PBS-T}$ . M4RT is a liquid medium commonly used in the transport of clinical specimens to the laboratory for qualitative microbiological procedures for viral and chlamydial agents. M4RT with no dilution can cause a decrease in capacitance ( $-0.48 \pm 0.035\% \cdot \text{min}^{-1}$ ), but for M4RT with 1:1,000 dilution or more in  $0.1 \times \text{PBS-T}$  its effect can be neglected ( $0.46 \pm 0.45\% \cdot \text{min}^{-1}$  at 1:1000 dilution). So dilution factors higher than 1:1000 are studied. To find out the optimal dilution factor to test, two clinical nasal swab samples (one positive and one negative) at various dilution factors from 1:100,000 to 1:1,000. Each sample is tested in triplicates, and each chip is tested with three dilutions in the sequence of 1:100,000, 1:10,000 and 1:1,000. Based on the sensor's readout (please refer to Fig. S2 in the supporting information), response reaches the highest at 1:10,000 dilution of positive sample. The 1:1000 dilution did not yield a larger response due to the saturation of the limited available binding sites on the electrode's surface. Nevertheless, 1:100,000 dilution is adopted instead of 1:10,000 since the response of sample at

1:100,000 dilution ( $-4.09 \pm 2.06\% \cdot \text{min}^{-1}$ ) is located around the median of the dose response line shown in Fig. 4. So 1:100,000 dilution is chosen in order to acquire a larger dynamic range in sensor response, desirable for clinical swab samples measurement in blind tests.

Blind tests for a panel of 20 nasal swab samples (10 positive, 10 negative) are conducted. All samples are 1:100,000 diluted with  $0.1 \times \text{PBS-T}$ . The threshold value is set at  $-0.40\% \cdot \text{min}^{-1}$ , which is also the LOD from previous tests with spiked samples, meaning that samples with a response more negative than  $-0.40\% \cdot \text{min}^{-1}$  will be considered as positive samples and others negative. As shown in Fig. 5a, nine out of ten positive and seven out of ten negative samples are correctly identified by ACEK capacitive sensors. A negative sample with influenza B virus is also correctly identified. All these samples are verified by RT-qPCR, yielding a sensitivity of 90% and specificity of 70% for the panel. Figure 5b shows a positive correlation between the capacitance change rate and PCR cycles number. Weak positive samples are chosen for this set of experiments. Among all the detected positive

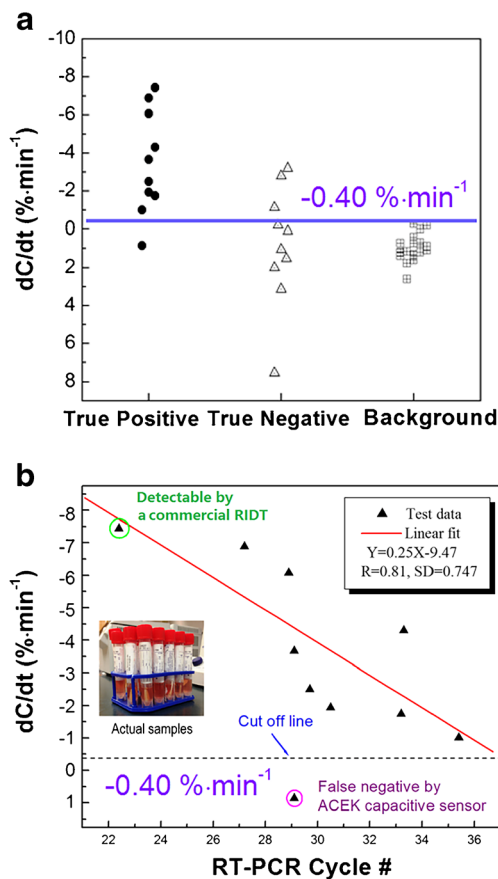


**Fig. 5** Comparison of results from ACEK capacitive sensors and those from commercial tests for a blind panel test of influenza virus A from nasal swabs. (a) Responses of all tested samples differentiated by the  $-0.40\% \cdot \text{min}^{-1}$  cut-off line (blue) and (b) correlation between PCR cycles and responses of samples determined as positive by ACEK capacitive sensor in blind tests. The strongest positive sample is the limit of a commercial rapid influenza test

samples, only the sample with the highest response can be detected by a commercial RIDT, which corresponds to 22 PCR cycles. ACEK capacitive sensor can detect virus level corresponding to 35 PCR cycles. There is a false negative corresponding to 29 PCR cycles. This is possibly due to error during dilution or the binding site on the virus not being exposed.

## Conclusions

This work presents a capacitive immunosensor based on ACEK for detection of specific virus particles from clinical samples. As a direct sensing method, this technology does not require any label, washing step, preconcentration or amplification for measurement. It is rapid, simple to operate, and work with clinical samples. Due to its high sensitivity, at a 1:100,000 dilution factor, the sensor still achieves a clinical sensitivity comparable to that of a RT-PCR with a 30 s response time. Dilution of clinical sample is needed to ensure the detection specificity. The sensor's specificity, which is 70%, can be further improved by optimizing the dilution solution. In addition, by changing the probe immobilized on the electrodes' surface, this sensor can be expanded to detect other protein biomarkers and pathogens. This sensor is highly promising for on-site disease detection and diagnosis.

**Acknowledgments** This work was supported by The University of Tennessee Research Foundation Maturation Fund, Center for Wildlife Health, and The University of Tennessee "Initiative for PON/POC Nanobiosensing".

**Compliance with ethical standards** The authors declare that they have no competing interests.

## References

- World Health Organization (2014) Influenza (Seasonal). <http://www.who.int/mediacentre/factsheets/fs211/en/>
- Pedersen JC (2008) Hemagglutination-inhibition test for avian influenza virus subtype identification and the detection and quantitation of serum antibodies to the avian influenza virus. In: Spackman E (ed) Avian influenza virus. Humana Press, Totowa, pp 53–66
- Poon LLM, Chan KH, Smith GJ, Leung CSW, Guan Y, Yuen KY, Peiris JSM (2009) Molecular detection of a novel human influenza (H1N1) of pandemic potential by conventional and real-time quantitative RT-PCR assays. *Clin Chem* 55:1555–1558. doi:10.1373/clinchem.2009.130229
- Leland DS, Ginocchio CC (2007) Role of cell culture for virus detection in the age of technology. *Clin Microbiol Rev* 20:49–78. doi:10.1128/CMR.00002-06
- ESPY M, Smith T, Harmon M, Kendal A (1986) Rapid detection of influenza virus by shell vial assay with monoclonal antibodies. *J Clin Microbiol* 24:677–679
- Chartrand C, Leeftang MMG, Minion J, Brewer T, Pai M (2012) Accuracy of rapid influenza diagnostic tests: a meta-analysis. *Ann Intern Med* 156:500. doi:10.7326/0003-4819-156-7-201204030-00403
- Yamanaka K, Saito M, Kondoh K, Hossain MM, Koketsu R, Sasaki T, Nagatani N, Ikuta K, Tamiya E (2011) Rapid detection for primary screening of influenza A virus: microfluidic RT-PCR chip and electrochemical DNA sensor. *Analyst* 136:2064. doi:10.1039/c1an15066a
- Loo JFC, Wang SS, Peng F, He JA, He L, Guo YC, Gu DY, Kwok HC, Wu SY, Ho HP, Xie WD, Shao YH, Kong SK (2015) A non-PCR SPR platform using RNase H to detect MicroRNA 29a-3p from throat swabs of human subjects with influenza A virus H1N1 infection. *Analyst* 140:4566–4575. doi:10.1039/C5AN00679A
- Ye WW, Tsang M-K, Liu X, Yang M, Hao J (2014) Upconversion Luminescence Resonance Energy Transfer (LRET)-based biosensor for rapid and ultrasensitive detection of avian influenza virus H7 subtype. *Small* 10:2390–2397. doi:10.1002/sml.201303766
- Nidzworski D, Pranszke P, Grudniewska M, Król E, Gromadzka B (2014) Universal biosensor for detection of influenza virus. *Biosens Bioelectron* 59:239–242. doi:10.1016/j.bios.2014.03.050
- Cui H, Li S, Yuan Q, Wadhwa A, Eda S, Chambers M, Ashford R, Jiang H, Wu J (2013) An AC electrokinetic impedence immunosensor for rapid detection of tuberculosis. *Analyst* 138:7188–7196. doi:10.1039/c3an01112g
- Li S, Cui H, Yuan Q, Wu J, Wadhwa A, Eda S, Jiang H (2014) AC electrokinetics-enhanced capacitive immunosensor for point-of-care serodiagnosis of infectious diseases. *Biosens Bioelectron* 51:437–443. doi:10.1016/j.bios.2013.08.016
- Rica R, Mendoza E, Lechuga LM, Matsui H (2008) Label-free pathogen detection with sensor chips assembled from peptide nanotubes. *Angew Chem Int Ed* 47:9752–9755. doi:10.1002/anie.200804299
- Birnbaumer GM, Lieberzeit PA, Richter L, Schirhagl R, Milnera M, Dickert FL, Bailey A, Ertl P (2009) Detection of viruses with molecularly imprinted polymers integrated on a microfluidic biochip using contact-less dielectric microsensors. *Lab Chip* 9:3549. doi:10.1039/b914738a
- Wu J, Ben Y, Chang H-C (2005) Particle detection by electrical impedence spectroscopy with asymmetric-polarization AC electroosmotic trapping. *Microfluid Nanofluid* 1:161–167. doi:10.1007/s10404-004-0024-5
- Yang K, Wu J (2010) Numerical study of in situ preconcentration for rapid and sensitive nanoparticle detection. *Biomicrofluidics* 4:34106. doi:10.1063/1.3467446
- Gao J, Sin MLY, Liu T, Gau V, Liao JC, Wong PK (2011) Hybrid electrokinetic manipulation in high-conductivity media. *Lab Chip* 11:1770. doi:10.1039/c1lc20054b
- Castellanos A, Ramos A, González A, Green NG, Morgan H (2003) Electrohydrodynamics and dielectrophoresis in microsystems: scaling laws. *J Phys Appl Phys* 36:2584–2597
- Wu J (2008) Advances of LOC-based particle manipulation by AC electrical fields. *Recent Pat Electr Eng* 1:178–198
- Pethig R (2013) Dielectrophoresis: an assessment of its potential to aid the research and practice of drug discovery and delivery. *Adv Drug Deliv Rev* 65:1589–1599. doi:10.1016/j.addr.2013.09.003
- González A, Ramos A, Green NG, Castellanos A, Morgan H (2000) Fluid flow induced by nonuniform ac electric fields in electrolytes on microelectrodes. II. A linear double-layer analysis. *Phys Rev E* 61:4019–4028. doi:10.1103/PhysRevE.61.4019
- Lian M, Islam N, Wu J (2007) AC electrothermal manipulation of conductive fluids and particles for lab-chip applications. *IET Nanobiotechnol* 1:36–43
- Yuan Q, Yang K, Wu J (2014) Optimization of planar interdigitated microelectrode array for biofluid transport by AC electrothermal effect. *Microfluid Nanofluid* 16:167–178. doi:10.1007/s10404-013-1231-8



24. Cui H, Cheng C, Lin X, Wu J, Chen J, Eda S, Yuan Q (2016) Rapid and sensitive detection of small biomolecule by capacitive sensing and low field AC electrothermal effect. *Sensors Actuators B Chem* 226:245–253. doi:[10.1016/j.snb.2015.11.129](https://doi.org/10.1016/j.snb.2015.11.129)
25. Chaurey V, Polanco C, Chou C-F, Swami NS (2012) Floating-electrode enhanced constriction dielectrophoresis for biomolecular trapping in physiological media of high conductivity. *Biomicrofluidics* 6:12806. doi:[10.1063/1.3676069](https://doi.org/10.1063/1.3676069)
26. Wu J, Ben Y, Battigelli D, Chang H-C (2005) Long-range AC electroosmotic trapping and detection of bioparticles. *Ind Eng Chem Res* 44:2815–2822. doi:[10.1021/ie049417u](https://doi.org/10.1021/ie049417u)
27. Cheng C, Wang S, Wu J, Yu Y, Li R, Eda S, Chen J, Feng G, Lawrie BJ, Hu A (2016) Bisphenol A sensors on polyimide fabricated by laser direct writing for onsite river water monitoring at attomolar concentration. *ACS Appl Mater Interfaces* 8:17784–17792. doi:[10.1021/acsami.6b03743](https://doi.org/10.1021/acsami.6b03743)
28. Rocha AM, Yuan Q, Close DM, O'Dell KB, Fortney JL, Wu J, Hazen TC (2016) Rapid detection of microbial cell abundance in aquatic systems. *Biosens Bioelectron* 85:915–923. doi:[10.1016/j.bios.2016.05.098](https://doi.org/10.1016/j.bios.2016.05.098)
29. Cui H, Cheng C, Wu J, Eda S (2013) Rapid detection of progesterone by commercially available microelectrode chips. *IEEE* 1–4. doi:[10.1109/ICSENS.2013.6688157](https://doi.org/10.1109/ICSENS.2013.6688157)
30. Chai C, Takhistov P (2010) Label-free toxin detection by means of time-resolved electrochemical impedance spectroscopy. *Sensors* 10:655–669. doi:[10.3390/s100100655](https://doi.org/10.3390/s100100655)
31. Liu X, Yang K, Wadhwa A, Eda S, Li S, Wu J (2011) Development of an AC electrokinetics-based immunoassay system for on-site serodiagnosis of infectious diseases. *Sensors Actuators Phys* 171:406–413. doi:[10.1016/j.sna.2011.08.007](https://doi.org/10.1016/j.sna.2011.08.007)
32. Park K, Akin D, Bashir R (2007) Electrical capture and lysis of vaccinia virus particles using silicon nano-scale probe array. *Biomed Microdevices* 9:877–883. doi:[10.1007/s10544-007-9101-3](https://doi.org/10.1007/s10544-007-9101-3)
33. Li S, Yuan Q, Morshed BI, Ke C, Wu J, Jiang H (2013) Dielectrophoretic responses of DNA and fluorophore in physiological solution by impedimetric characterization. *Biosens Bioelectron* 41:649–655. doi:[10.1016/j.bios.2012.09.036](https://doi.org/10.1016/j.bios.2012.09.036)
34. Lin X, Cheng C, Terry P, Chen J, Cui H, Wu J (2016) Rapid and sensitive detection of bisphenol A from serum matrix. *Biosens Bioelectron*. doi:[10.1016/j.bios.2016.12.024](https://doi.org/10.1016/j.bios.2016.12.024)